IJCTA, 9(29), 2016, pp. 231-237

A Single Phase Photovoltaic Microinverter with Soft-Switching Flyback Converter

R. Bhaskara rao* J. Sivavara prasad and K.R.L. Prasad*****

Abstract : This paper presents a single-phase microinverter for a grid-connected PV system. It consists of an isolated step up *dc–dc* converter using an active-clamp circuit with a series resonant voltage doubler and current controlled inverter. Inverter output current is controlled such that MPPT is achieved. Output voltage of dc-dc stage is maintained constant at a value greater than peak grid voltage. The active-clamp circuit provides zero-voltage switching (ZVS) turn-on, and limits switch voltage stress. A series-resonant voltage double removes the reverse-recovery problem of the rectifier diodes. Only single switch is modulated in inverter stage. Thus, the proposed PV microinverter has the structure to minimize power losses. A 400watt micro inverter is designed and simulated to conform the validity.

Keywords : Micro inverter, Voltage doubler, MPPT, ZVS, ZCS, Active clamp.

1. INTRODUCTION

The increasing energy shortages and the exhaustion of global resources, leads the current researchers to concentrate on renewable energy[1]. Despite the fact that PV energy is known as one of the great alternative sources, the PV system costs more. Therefore, the cost and energy efficiency of the PV system and the extracted power from the PV panel should be improved. Thus, it is essential for a PV system to have the high-efficiency inverter and the maximum power point tracking (MPPT) control technique, which extracts the maximum power from the PV panel. Based on the connection method of PV modules, the PV system is classified into the centralized system, the string system, and the microinverter[2]. Among them, the microinverter offers high efficiency of MPPT according to the individual module control. But, it is still costly to be used widely. Therefore, in order to reduce cost and improve efficiency of the microinverter, various studies are being carried out[3]-[5]. The output voltage of a PV panel is generally supplied by a low-level dc voltage, so a high voltage gain inverter is needed to meet high voltage loads. The simple boost converter has been proved to be insufficient in providing high step-up ratios in an efficient way, due to the high current and voltage stress on the switch and the severe diode reverse recovery losses, when operating in continuous conduction mode. Thus, the PV inverter topology with galvanic isolation is preferred for the microinverter. The flyback topology[6] of the conventional microinverter is typically provides relative simplicity of the circuit structure, ease of control, and minimal number of switching devices compared to other topologies. However, there are drawbacks such as switching losses of the switch and reverse-recovery losses of the diodes. Furthermore, the high turn ratio of the transformer increases the leakage inductance of the transformer, and its large inductance deteriorates the system efficiency. Due to the lower utilization of the transformer, the flyback topology is limited for low wattages. Thus, the increased power rating of the microinverter is required to cope with large power rating of the PV panel and to lower the cost per watt of the microinverter.

* Laki Reddy Bali Reddy College, mylavaram, Andhra Pradesh, India. Email: baskar.ravada@gmail.com,

** Laki Reddy Bali Reddy College, mylavaram, Andhra Pradesh, India Email:janapatisivavaraprasad@gmail.com

2. RESEARCH METHOD

The circuit configuration of the *dc–dc* stage is shown in Fig 2. The *dc–dc* stage consists of an active-clamp circuit in the primary side and the series-resonant voltage doubler in the secondary side of the transformer T1. The active-clamp circuit is composed of a switch S1, a switch S2, and a clamp capacitor Cclamp. This circuit limits the voltage across the switch S1 and regenerates the energy stored in the leakage inductance Lleak. Then, the switches S1 and S2 are operated complementarily with the zero-voltage switching (ZVS) turn-on. In the secondary side of the transformer T1, rectifier diodes Dr1 and Dr2 and a resonant capacitor Cr represent the series-resonant voltage doubler. This circuit provides the resonant-current paths of the power transfer, regardless of the main switch state. In particular, the resonant current formed by leakage inductance of the transformer and the resonant capacitor removes the reverse-recovery problem of the secondary rectifier diodes Dr1, Dr2. Fig 2.Shows the equivalent circuit of the dc–dc stage. The active-clamp circuit and the series-resonant voltage doubler can be analyzed in the six operation modes, according to the conduction states of the switches and diodes during one switching period Ts, dc.

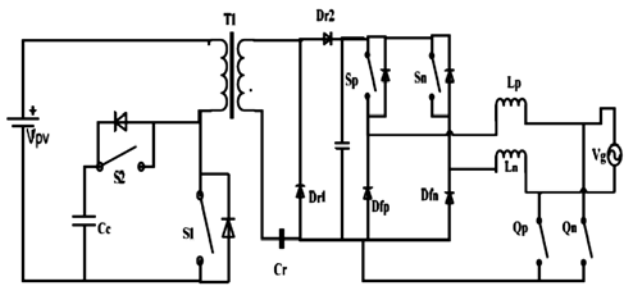

Fig. 1. Proposed microinverter.

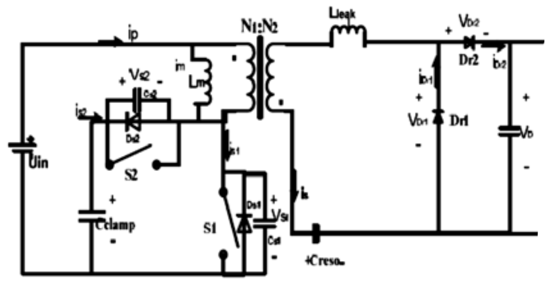

Fig. 2. Equivalent circuit of the dc-*dc* stage.

Mode (*i*): When switch S_1 is closed at time t_1, the voltage V_{s1} across the switch S_1 becomes zero, and the primary current i_p of the transformer flows. When, the input voltage U_{in} equals the voltage across magnetizing inductance Lm, the magnetizing current iLm increases linearly. In addition, the series resonance occurs between the capacitor C_{reso} and the leakage inductance L_{leak} of the transformer. The voltage across the leakage inductance L_{leak} is the difference between the secondary voltage nU_{in} and the resonant capacitor voltage V_{creso}. Thus, the secondary current is of the transformer flows through the rectifier diode Dr1 with the resonance of the positive current.

Mode (*ii*): At time t_2 secondary current is becomes zero, such that primary current is equal to magnetizing current i_{Lm}. Therefore ip increases linearly.

Mode (*iii*): The rectifier diode D_{r1} and the switch S_1 are turned off. Since the secondary current i_{Dr1} is already zero in Mode2, the reverse-recovery loss of the rectifier diode D_{r1} is removed. At the same time, the output capacitor C_{s1} of the switch S_1 is charged, and the output capacitor C_{s2} of the switch S_2 is discharged.

Mode (*iv*): At the end of Mode3, the voltage V_{s2} across the switch S_2 is zero, and the primary current i_p flows through the antiparallel diode of the switch S_2. Thus, the ZVS turn-on of the switch S_2 is achieved. Then, the voltage across magnetizing inductance Lm equals Uin − Vc, and the magnetizing current i_{Lm} decreases linearly. At the same time, the rectifier diode D_{r2} is in the on-state.

Mode (*v*) : Since the secondary current i_{Dr2} is already zero in Mode 4, the reverse-recovery loss of the rectifier diode Dr2 is removed. Similar to Mode3, the rectifier diode Dr2 achieves the zero-current switching (ZCS) turn-off. As the secondary current i_s becomes zero, the primary current i_p and the magnetizing current i_{Lm} are linearly decreased.

Mode (*vi*) : The switch S_2 and the secondary side diodes Dr1 and Dr2 of the transformer are in the off-state. The output capacitor C_{S1} of the switch S_1 and the output capacitor C_{S2} of the switch S_2 are discharged and charged, respectively. At the end of mode6, the voltage v_{S1} across the switch S_1 is zero, and the primary current ip flows through the antiparallel diode of the switch S_1.Thus, the ZVS turn-on of the switch S_1 can be achieved in mode 1.

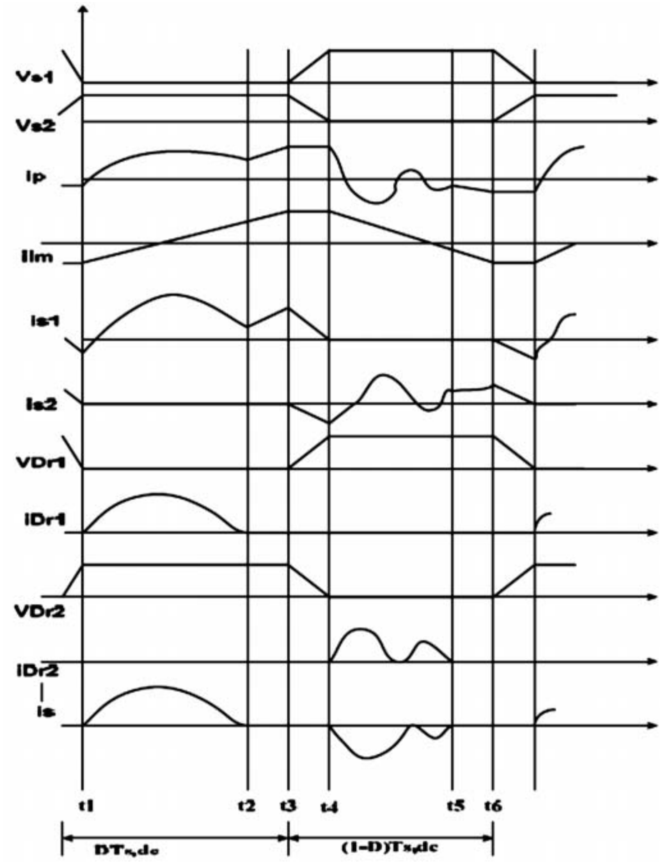

Fig. 3. Theoretical waveforms of *dc-dc* stage.

The proposed inverter is based on two step-down converters. In contrast with the conventional full-bridge structure, the inverter uses two switches instead of four switches. The two switches Qp and Qn are operated complementarily at a grid frequency that depends on the grid voltage polarity. In the operation of the inverter, the input voltage V_d of the inverter stage is constantly controlled by the *dc–dc* stage at higher value than the peak grid voltage. For the positive grid voltage, the positive path selector Qp of the grid current is turned on, and the switch Sp is modulated by the control of the grid current. When the switch Sp is turned off, the freewheeling path occurs through the diode D_{fp}. Thus, a single switch Sp or Sn is modulated every half-period of the grid voltage. Thus, the inverter is operated without a shoot-through problem.

3. DESIGN CONSIDERATIONS

1. Magnetizing inductance Lm

Writing the average inductor current equation for total time period and solving for Lm, gets as follows

$$\mathrm{Lm} = \frac{(1-\mathrm{D})^2\mathrm{R}}{2f}\left(\frac{\mathrm{N1}}{\mathrm{N2}}\right)^2 \tag{1}$$

An additional dead-time period is introduced between the turn on and turn off transitions of Q1 and Q2. During the dead-time, primary current flow remains continuous through the body-diode of the P-channel AUX MOSFET, Q2, or the main MOSFET, Q1. This is commonly known as the resonant period in which the conditions are set for zero voltage switching (ZVS).

$$\text{Tdelay} = \frac{\pi}{2}\sqrt{L_{eq} \times 2 \times C_{ds}} \quad (2)$$

2. Leakage inductance Llk & Resonant capacitor Cr

The series resonance occurs between the capacitor C_{reso} and the leakage inductance L_{leak} of the transformer. The voltage across the leakage inductance Lleak is the difference between the secondary voltage nUin and the resonant capacitor voltage V_{Cres}o. Thus, the secondary current is of the transformer flows through the rectifier diode Dr1 with the resonance of the positive current.

The resonant angular frequency ωr1 and the impedance Zr1 of the resonant circuit are given by

$$Z_{r1} = \sqrt{\frac{L_{leak}}{C_{reso}}}$$

$$\omega_{r1} = \frac{}{\sqrt{L_{leak}C_{reso}}}$$

Since the resonant sinusoidal value sin (ω_{r1} DT, *dc*) at the on-time DTs, *dc* must be negative to achieve for the ZCS turn-off of the rectifier diodes, the following equation is obtained as

$$\omega_{r1}\, DT_{s,dc} > \pi$$

Thus, the resonant capacitor Cr of the series-resonant voltage doubler is given by

$$C_{reso} < \frac{D^2 T_{s,dc}^2}{\pi^2 L_{leak}}$$

3. Clamp capacitor C_{clamp}

A simplified method for approximating C_{clamp}, is to solve for C_{clamp}, such that the resonant time constant is much greater than the maximum off-time.

$$2 \times P \times f\sqrt{Lm \times C_{clamp}} > 10 \times t_{off(max)}$$

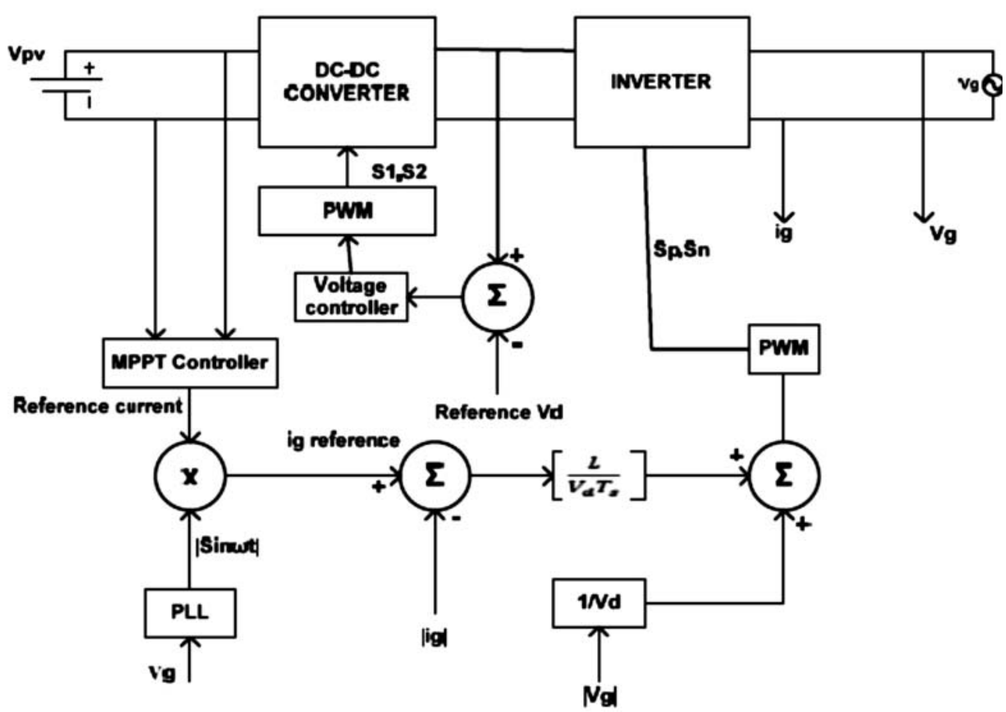

Fig. 4. Control block diagram of proposed micro inverter.

Where Lm is transformer magnetizing inductance and $t_{off(max)}$ is the maximum off-time. By dividing both sides of by the total period, T, and solving for Cc in terms of known design parameters as follows

$$C_{clamp} > \frac{10 \times (1 - D_{min})}{Lm \times (2 \quad)}$$

In the inverter stage, the inductance L of Lp and Ln is calculated by using the buck converter steady state equations. Thus, the inductance L should satisfy as follows

$$L > \frac{\left(1 - \frac{Vg}{Vd}\right)^2}{2 \times f_{sw}} \times R_L$$

Where Vg is the maximum value of grid voltage, and f_{sw} is the switching frequency of inverter.

Table 1. Specifications of proposed microinverter.

Parameters	***Values***
Input voltage	65volts
Rated power	400watt
Switching frequency of dc stage	50Khz
Switching frequency of inverter	16Khz
Clamp capacitor	2.2uF
Resonant capacitor	2.4uF
Turns ratio	1:4
Magnetising inductance	20uH
Inverter filter inductors	15mH

4. RESULTS

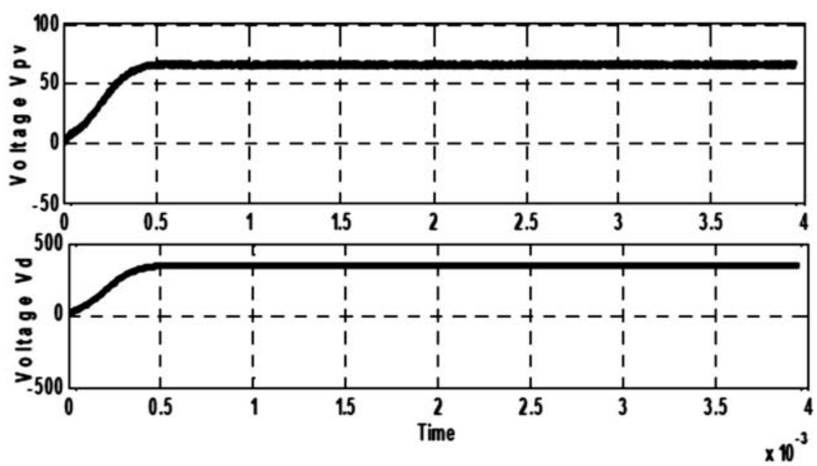

Fig. 5. Shows boosting of input voltage.

A 400-W microinverter was designed and simulated in MATLAB/SIMULINK software with the component values obtained from the design procedure aforementioned are listed in Table I. Fig 5 shows that flyback converter boosts the input voltage 65v to 350v. It is shown in fig 6 and 8 that, during the turn ON, the gating voltage for the primary switches is applied only after voltage has become zero. Thus ZVS turn on is achieved. An active clamp circuit is used to reduce the voltage spikes observed across the primary switches during turn OFF in the simulations. Fig 7 shows that rectifier diodes have no reverse-recovery problem due to ZCS turn-off. Figure 9 shows Grid voltage Vg and grid current ig. From Fig 9 it is observed that 350v DC is converted to AC and connected to single phase grid. The switches Qp and Qn act as grid driver, which ensures frequency matching between grid and inverter. Efficiencies of both DC-DC and DC- AC stages are measured for different values of input voltages in the range 45V to 75V. It is found that at input voltage of 65V maximum efficiency is achieved.

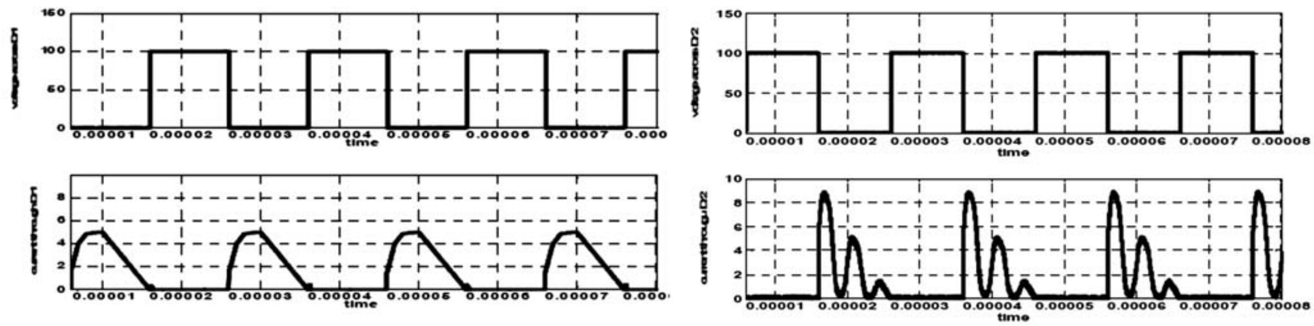

(*a*) (*b*)

Fig. 6. ZCS turn-off rectifier diodes.

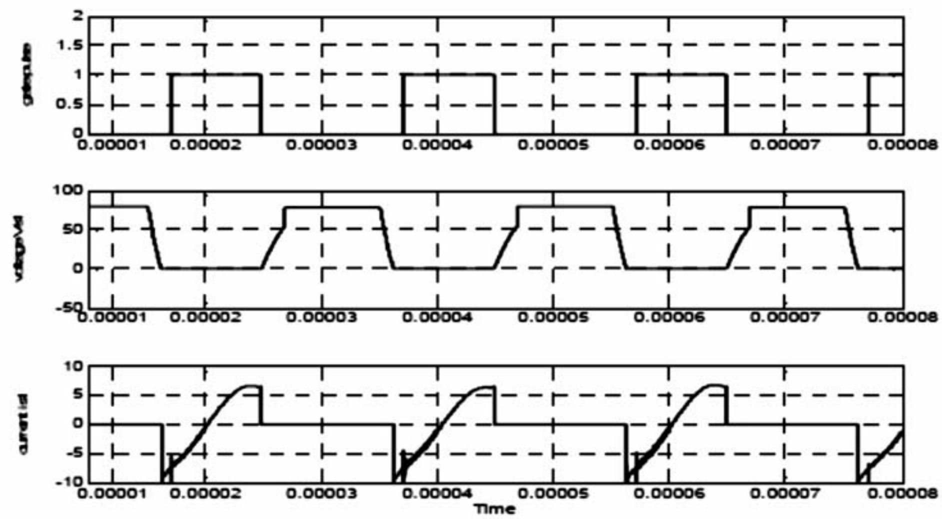

Fig. 7. Gate pulse ,voltage, current of S1.

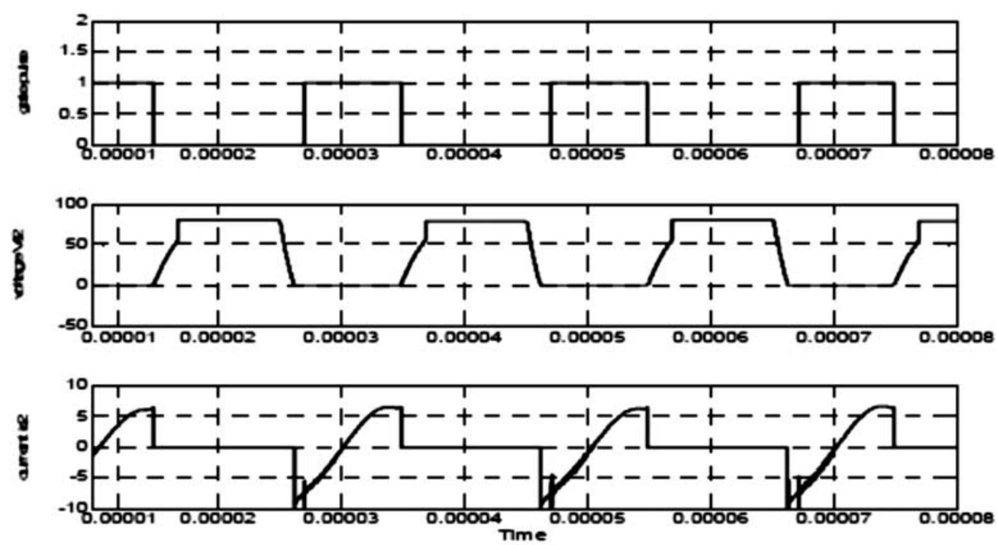

Fig. 8. Gate pulse ,voltage, current of S2.

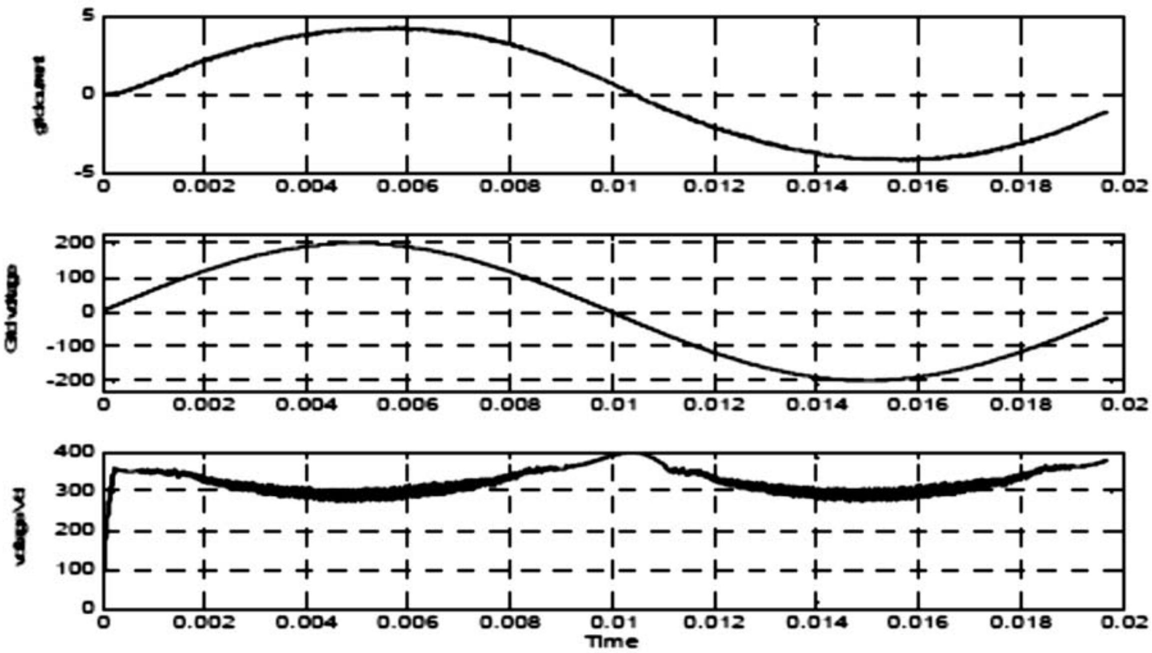

Fig. 9. Grid voltage and Grid current.

5. CONCLUSION

This paper illustrates a single phase microinverter with soft-switching step-up converter. The active-clamp circuit offers the soft switching of the primary-side switches and reduces the voltage stress by clamping the voltage spike across the switches. Its series-resonant voltage doubler provides the ZCS turn-off of the rectifier diodes. Hence switching power losses are minimized. A 400 watt microinverter is designed and simulated to conform the validity. The efficiencies of flyback converter and micro inverter with and without active clamp circuit are measured for different values of input voltage Vpv and for different loads. It is observed that at 65v and 400watt efficiency of flyback with active clamp is 97.52% and micro inverter is 94.83%.

6. REFERENCES

1 N. Sukesh, M. Pahlevaninezhad, and P. K. Jain, “Analysis and implementation of a single-stage flyback PV micro-inverter with softvswitching,”IEEE Trans. Ind. Electron., vol. 61, no. 4, pp. 1819–1833, Apr. 2014.M. Young, The Technical Writer’s Handbook. Mill Valley, CA: University Science, 1989.

2. Y. Xue, L. Chang, S. B. Kjær, J. Bordonau, and T. Shimizu, “Topologies of single-phase inverters for small distributed power generators: An overview,” IEEE Trans. Power Electron., vol. 19, no. 5, pp. 1305–1314, Sep. 2004K. Elissa, “Title of paper if known,” unpublished.

3. R. W. Erickson and A. P. Rogers, “A microinverter for building-integrated photovoltaics,” in Proc. IEEE Appl. Power Electron. Conf. Expo.,Feb.2009, pp. 911–917.

4. W. Y. Choi, “High-efficiency DC-DC converter with fast dynamic response for low-voltage photovoltaic sources,” IEEE Trans. Power Electron., vol. 28, no. 2, pp. 706–716, Feb. 2013.

5. D. Meneses et al., “Single-stage grid-connected forward microinverter with constant off-time boundary mode control,” in Proc. IEEE Appl. Power Electron. Conf. Expo., Feb. 2012, pp. 568–574.

6. Power Electronics: Essentials & Applications, L. Umanand.